



Research article

Innovative spiral electrode configuration for enhancement of electrocoagulation-flotation

Ehsan Jafari^a, M. Reza Malayeri^{b,*}, Heike Brückner^a, Thomas Weimer^c, Peter Krebs^a

^a Institute of Urban and Industrial Water Management, Technische Universität Dresden, Germany

^b Department of Chemical Engineering, Shiraz University, Iran

^c Department of Research and Development, Spiraltec GmbH, Germany



ARTICLE INFO

Handling Editor: Raf Dewil

Keywords:

Electrode configuration
Electrocoagulation process
Electro-flotation
Energy consumption
Removal efficiency

ABSTRACT

The performance of electrocoagulation-flotation (ECF) process can profoundly be affected by the reactor design and electrode configuration. These may, in turn, influence the removal efficiency, flow hydrodynamic, floc formation, and flotation/settling characteristics. The present work aimed at developing a new spiral electrode configuration to enhance the ECF process. To do so, the impacts of parameters such as energy consumption, removal efficiency of the contaminants from industrial wastewater with a composition of turbidity, emulsified oil, and heavy metals (Si, Zn, Pb, Ni, Cu, Cr, and Cd), as well as stirring speed and foaming have been investigated. Comparison was also made between the experimental results of the new electrode configuration with the conventional rectangular cell with plate electrode configuration with the same volume and electrode surface area. The findings revealed that energy consumption of the spiral electrode configuration within the operating times of 10, 20, 30, 32, 48, and 70 min, was approximately 20% lower compared to that of the conventional ECF. Moreover, the maximum and minimum removal efficiency of 97% and 60% were obtained for turbidity and TOC for the stirring speed of 500 rpm and Reynolds number of 10,035, respectively. Finally, the formed gas bubbles tilted toward the center due to the enhanced flow hydrodynamic which resulted in substantial reduction of foam formation.

1. Introduction

Strict environmental legislations and regulations concerning the discharge of wastewater are continuously increasing (Mouedhen et al., 2008). Many industrial processes (e.g. metal processing industry) demand tremendous amount of water, which may ultimately be converted into wastewater. This situation is not sustainable given the scarcity of water in many parts of the world. Thus, wastewater needs to be treated properly, in order to obtain a purity level for reuse in the industrial processes or other purposes (Barrera-Díaz et al., 2012).

Electrocoagulation-flotation (ECF) can potentially be utilized in industrial wastewater treatment by applying a current to the electrodes from an external power source that produces metal coagulant in-situ by dissolving sacrificial electrodes (Vik et al., 1984). At the negatively charged cathode, water is electrolyzed to produce OH^- and $\text{H}_2(\text{g})$ (Mansoorian et al., 2014). In general, aluminium (Al) or iron (Fe) are commonly used as EC electrodes (Chen, 2004) (Mohammadi et al., 2017). The utilization of Al or Fe electrodes depends primarily on the

solution's pH. According to the Al/Fe pH diagram, the suitable pH for formation of $\text{Al}(\text{OH})_3$ ranges from 5.5 to 7.5 and for the Fe electrode, an alkaline pH would be sufficient. Electrocoagulation-flotation is capable of reducing waste production in wastewater treatment due to vertical electrode configuration, in which, the gas bubbles that are formed on the cathode could then attach to contaminants before rising to the surface, under which higher removal efficiency would be expected. In horizontal EC configuration though, the reactor depth is not enough, causing meagre impact of gas bubbles. The ECF process has successfully been applied for removal of pollutants, and also turbidity as a measure of water clarity that can be affected by various pollutants (Zongo et al., 2009) (Solak et al., 2009), emulsified oil (Canizares et al., 2008), heavy metals (Heidmann and Calmano, 2008), dyes (Phalakornkule et al., 2010) (Zidane et al., 2008), and phenols (Adhoum and Monser, 2004) (Ugurlu et al., 2008) from synthetic and real wastewaters.

The ECF technique would have several advantages to overcome the drawbacks of other treatment processes (Ingelsson et al., 2020), e.g. low sludge production, low maintenance costs, and treatment of multiple

* Corresponding author.

E-mail address: malayeri@shirazu.ac.ir (M.R. Malayeri).

<https://doi.org/10.1016/j.jenvman.2023.119085>

Received 30 May 2023; Received in revised form 9 August 2023; Accepted 30 August 2023

Available online 25 September 2023

0301-4797/© 2023 Elsevier Ltd. All rights reserved.

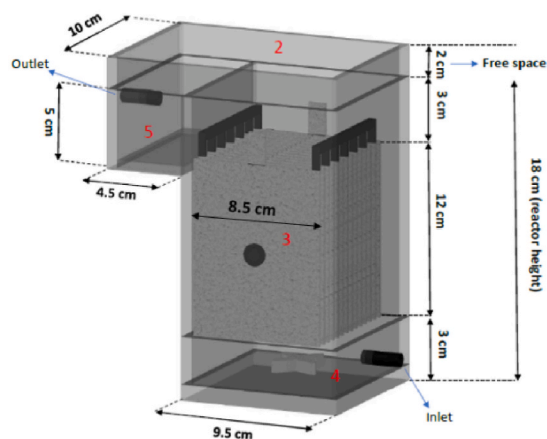


Fig. 1. Schematic and constructed rectangular cell configuration with plate electrodes.

contaminants in one pass (Bandaru et al., 2020). Nevertheless, it is still prone to some drawbacks in long term operation (Ingelsson et al., 2020) such as precipitation and deposition of solids on the electrodes over time (passivation problems), or non-uniform electrode consumption which may be caused as a result of the non-uniform potential and current density on the electrode surface (Bandaru et al., 2020) (Garcia-Segura et al., 2017) (Müller et al., 2019).

Higher ECF efficiency is closely associated with the dissolution of anode, hence the production of aluminium metal ions which can be strengthened by increasing the number of electrodes to get a larger active surface (Brahmi et al., 2019a) (Hakizimana et al., 2017). This would, in turn, prevent the generation of a significant ohmic resistance, which would not only depend on the number of electrodes, but also the configuration of electrodes (Brahmi et al., 2019a). Although the most common design of ECF reactor in conventional applications is open-vertical-plate electrode configuration in a rectangular cell but mixing is the main drawback of this cell geometry, as vertical electrodes may serve as barrier which may disrupt the flow hydrodynamics (Hakizimana et al., 2017).

The overall performance of the ECF process can be affected by its design which may influence the operating parameters such as removal efficiency, flow pattern, flocs formation, and flotation/settling characteristics (Hansen et al., 2007). The removal of contaminants is closely associated to the production of coagulants inside the ECF reactor, indicating the performance of the mass transport of Al^{3+} ions. Thus, to improve the formation of coagulants, a turbulent flow regime would be desired to enhance the mixing of dissolved metal and hydroxide as such

that the removal efficiency of ECF would be expected to increase (Hansen et al., 2007) (Noorzalila Muhammad et al., 2019) (Trinh et al., 2021).

Rectangular cells still dominate the market and can be utilized for plate electrodes. Thus the foremost common design in typical applications is the open vertical-plate cell, which is also equipped by a settler. Vertical electrodes are similarly spaced in parallel, which would make the scale-up much simpler. Furthermore, this configuration provides easier cleaning of electrodes, but the main drawback of this cell geometry is the poor and insufficient mixing (Hansen et al., 2007). In a conventional rectangular electrode configuration, the flow circulation between the electrode plates is often inadequate. The limited circulation, in turn, can lead to a range of complications, most notably, fouling on the anode electrode. In fact, in the electrocoagulation process, the anode plays a crucial role. As soon as an electrical current is applied, the anode, typically made of a metal such as aluminium or iron, releases metal ions into the water. These ions interact with contaminants, leading to coagulation. This reaction forms larger particles or 'flocs,' which can then be easily separated from the water. The deposition of anode occurs when particles, impurities, or precipitated secondary products accumulate on the surface. Accordingly, anode performance can be affected severely, reducing its effectiveness in releasing metal ions and thereby reducing electrocoagulation efficiency. In addition, the flow may not be strong enough to push out the generated gas bubbles from the cathode. This is because the accumulation of hydrogen bubbles around the electrodes is shown to cause high internal resistance between the electrodes, impeding ion migration and ultimately reducing the

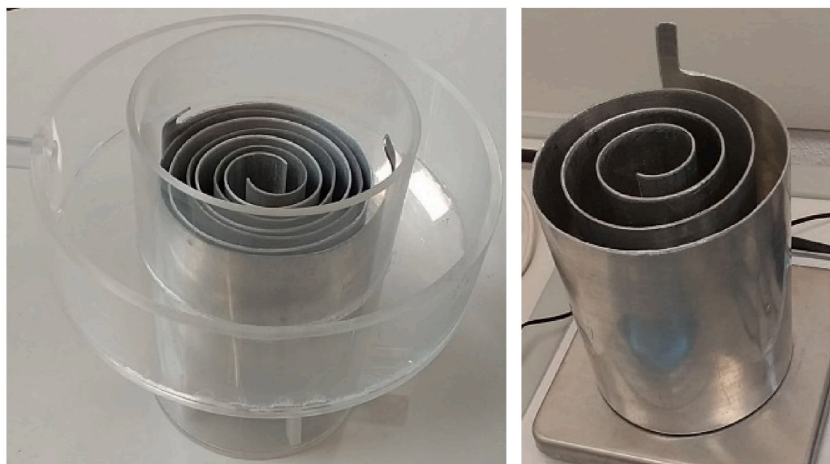
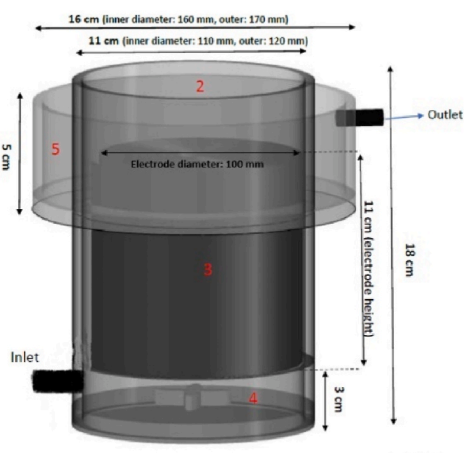


Fig. 2. Schematic and constructed cylindrical cell configuration with spiral electrodes.

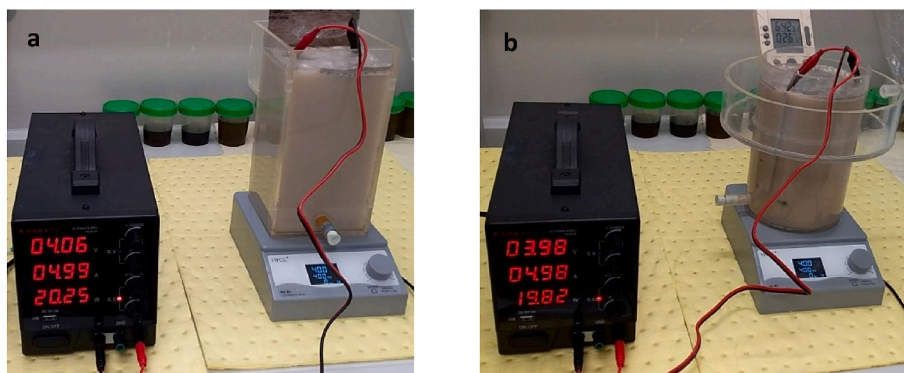


Fig. 3. a) Conventional experimental setup, b) Innovative experimental setup.

efficiency of the EC cell (Noorzalila Muhammad et al., 2019). Gas bubbles, which are mainly produced by oxygen and hydrogen and are formed during the electrolysis process on the cathode, could also form a lot of foam as time elapses. The foam will significantly decrease the efficiency of the ECF process, and the voltage can rise sharply, thereby increasing the energy consumption of the process (Jafari et al., 2023).

Given the above-mentioned operating drawbacks of the parallel plate electrode configuration, a new cylindrical cell configuration with spiral electrodes is proposed and designed in this study. The main notion was to enhance the ECF process in terms of contaminant removal efficiency and energy consumption. Therefore, the objectives of this study were to 1) design and implement a cylindrical ECF reactor with spiral electrodes; 2) assess the performance of the new ECF configuration in terms of contaminant removal efficiency and energy consumption; 3) compare the performance of the new design against a conventional rectangular ECF reactor with parallel plate electrode configuration. These objectives have been followed by treatment of industrial wastewaters which contained turbidity, emulsified oil, and heavy metals (Si, Zn, Pb, Ni, Cu, Cr, and Cd). The comparison of two ECF configurations were also made in terms of removal efficiency, flow regime, energy consumption, and foam formation.

2. Materials and methods

2.1. Experimental setup

The conventional ECF cell was made up of 1.71 L rectangular acrylic glass. It was used in this study for two reasons, i) it is widely used in industrial electrocoagulation processes; and ii) for the sake of comparison with the new cylindrical cell with spiral electrodes. Plate aluminium electrodes (alloy EN AW-1050A which is the purest form of aluminium with purity of 99.5%), were used in connection with an outer part for collection of probable formed foam (Fig. 1). To compare the test results, a cylindrical cell with two aluminium electrodes in spiral shape (anode and cathode) with the same volume, material, and electrode surface area ($S = 714 \text{ cm}^2$ for both anode and cathode) was constructed (Fig. 2). A distance of 5 mm between the electrodes was considered for

both configurations to reduce energy consumption and increase the removal efficiency. The experimental setup has been presented in Fig. 3, in which the ECF cells (a: conventional experimental setup and b: Innovative experimental setup) were placed on a magnetic stirrer and the supplied DC (Direct Current) power was connected to the electrodes at a given operating time. In continuous mode, the feed flows to the cell through the inlet pipe, located in the bottom, which would then be drained from the outlet pipe. Nevertheless, in this study, the inlet and outlet pipes were closed so that, the cells would only be operated in batch mode as the first phase, to accurately estimate the coagulant concentration, energy consumption, and formation of foam for a specified operating time. In the future, a continuous mode will also be investigated. The characteristics of both ECF configurations are as follows:

1. Total volume of Reactor: 1.71 L
2. Volume of free space (top of the reactor): $0.19 \times 10^{-3} \text{ m}^3$
3. Volume of electrode space (solid + liquid): 1.14 L
4. Volume of stirrer and primary settling space (bottom of the reactor): 0.285 L
5. Volume of foam collection part: 0.225 L for conventional and 0.53 L for cylindrical ECF
6. Volume of Al- electrodes (solid): $0.285 \times 10^{-3} \text{ m}^3$
7. Total electrode surface: 1428 cm^2 (anode: 714 cm^2 , cathode: 714 cm^2)

It should also be pointed out that, when calculating the current density, only the area of one electrode would be taken into account provided that the area of the anode is equal to that of cathode.

2.2. Sampling and analytical measurements

The wastewater, used in this work, was collected from a major metal manufacturer in Germany. To consider the dependency of removal efficiency with concentration, the feed was diluted with deionized water then analyzed according to Table 1. The major characteristics of this feed, as presented in Table 1, include turbidity which was analyzed for

Table 1
Feed analysis of different concentrations.

Parameters	Cr	Cu	Pb	Zn	Si	TN	TOC	Turbidity	pH
Unit/conc.	mg/L	NTU							
Feed 1 (no dilution)	10.1	5.54	2.22	13.6	154	2189	31,895	15,300	8.9
Feed 2 (30% W+70% F)	5.19	2.99	1.21	7.21	119	1045	15,015	8410	8.7
Feed 3 (50% W+50% F)	3.61	2.14	0.84	5.33	76.6	745	10,740	5700	8.8
Feed 4 (70% W+30% F)	2.13	1.51	0.45	3.16	33.6	434	6135	3115	8.8
Feed 5 (80% W+20% F)	1.49	1.18	0.29	2.40	22.2	304	4205	1990	8.9
Feed 6 (90% W+10% F)	0.80	0.83	0.15	1.31	12.2	158	2270	1096	8.8

•F: feed, W: deionized water

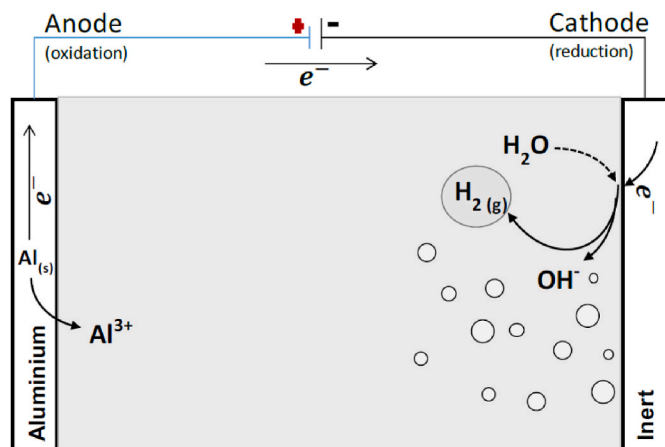


Fig. 4. Sketch of Eq. (1) and Eq. (2) inside the EC reactor. The inert electrode is usually the same material as anode, adopted from (Lima, 2019).

remaining colloidal particles by a turbidity meter (model Turb 430 IR produced with Xylem, Germany), total organic carbon that was measured by TOC (Total Organic Carbon) V_{CPH} Shimadzu and method of DIN EN 1484, and heavy metals (Cr, Cu, Pb, Zn, and Si) with ICP-OES Spectra (Inductively Coupled Plasma Optical Emission spectroscopy) Avio 200 and method of EN ISO 11885 (E 22). The major composition of total nitrogen (TN) was ammonium which is a weak acid and serves as buffer solution. Accordingly, no change in pH was expected with the dilution of solution.

2.3. Experimental procedure

A power supply (PS-3010F, 30V, 10 A) provided DC current in galvanostatic mode. To avoid the occurrence of passivation, prior to each test, the electrodes were washed with 2% HCl for about 1 min then rinsed with deionized water. The electrodes were examined before and after washing and rinsing with the diluted 2% HCl and water to examine if the surface roughness has changed. In many instances though, no such changes were noted but the electrode was replaced if the changes were noticeable. In total, 60 runs were carried out in this work, out of which 7 runs as calibration tests and 53 runs as the main tests. The influential experimental parameters in our study were the current density (CD), operating time, and stirring speed which were measured before and after each test. Other parameters such as pH, electrolyte conductivity, and temperature were measured in order to monitor the process. The experiments were designed as such that each parameter varied systematically while keeping others constant, which allowed to isolate the impact of each parameter on the desired objective function.

The solution volume in all tests was equal to 1300 ml to make sure that the electrodes were fully covered by the solution. As volume changes can affect a variety of system parameters, thus the same initial volume of 1300 ml was maintained in all runs to ensure consistency and also to facilitate better comparison of the results. Based on the feed concentrations (Table 1), a range of current from 3 A to 10 A was applied to determine the optimum current density for each concentration. After electrolysis, the electrodes were removed and the reactor was used as a settling tank so that the samples were taken after 15 min once the ECF was turned off. The purpose of this settling period was to allow larger particles or 'flocs' which were formed during the electrocoagulation process to settle. This made the subsequent filtration process more efficient by reducing the burden on the filter and preventing potential clogging issues. Thereafter, the solution was filtered with a paper filter size of 20 μm followed by the one with 5 μm . The utilization of a settling tank before filtration was due to the formation of flocs which may take a while. This has to be carried out in a separate reactor, where the flocs had ample time to become bigger. The filtration efficiency will be

reduced if one filters the outflow after the ECF, since some flocs are small enough to pass through the filter. For the sake of consistency, several selected tests were repeated to make sure that the results are reproducible. It should be noted that during experiments, only negligible deposition was observed on the stir bar which, nevertheless, did not noticeably impact the overall results of electrocoagulation process.

3. Results and discussion

3.1. Theory

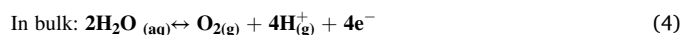
In ECF, as soon as an external direct current is applied, then a sequence of electrochemical reactions would take place at the anode and cathode of an electrolytic cell. ECF involves the generation of in-situ metal coagulants by electrolytic dissolving sacrificial anode materials (aluminium or iron) (Barrera-Díaz et al., 2011). The metal used in this research was aluminium. The anodic process, in turn, involves the oxidative dissolution of aluminium into aqueous solution as expressed in Eq. (1) and Fig. 4. On the cathode, the reductive dissociation of water occurs as shown in Eq. (2) and Fig. 4. The term "inert" in Fig. 4 was used to underline that the primary electrochemical reactions occur on the anode. Nonetheless, the aluminium cathode may also subject to negligible dissolution as observed in this study.



The cathodic reaction (Eq. (2)), has three important implications that can be used to improve the ECF process so then higher pollutant removal efficiency would be expected:

- 1) reaction in Eq. (2) provides hydroxyl ions (OH^{-}) which would then react in the bulk solution with aluminium cations to form coagulants;
- 2) the produced hydrogen gas (H_2) contributes to the destabilization of colloidal particles leading to flocculation, and finally
- 3) pollutants can be floated by their adhesion onto small bubbles formed by hydrogen evolution (electroflotation) (Burns et al., 1997), (Poon, 1997), (Casqueira et al., 2006).

It should be also noted that in EC there are two anodic reactions, the primary reaction that is discussed in Eq. (1), and secondary reactions which in the EC related literature, have received least attention. The secondary reactions, as underlined below, in the current of an adequately high potential are likely to occur at the anode present in wastewater, especially oxygen evolution, such as direct oxidation of organic compounds such as H_2O or Cl_2 (Brahmi et al., 2015).



Aluminium ions (Al^{3+}), produced by electrolytic dissolution of the anode which may serve as coagulant reagent, could hydrolyze and form mononuclear complexes according to the following sequence (Barrera-Díaz et al., 2011):



Reactions (5) to (8) represent a sequence of progressive hydrolysis of Al^{3+} . Reactions (6) and (7) show the sequential steps in the hydrolysis of aluminium ions in water. In particular, reaction (6) shows the hydrolysis of $\text{Al}(\text{OH})^{2+}$ to form $\text{Al}(\text{OH})_2^{+}$ and a proton (H^{+}), while reaction (7) shows the subsequent hydrolysis of $\text{Al}(\text{OH})_2^{+}$ to form aluminium hydroxide (Al

Table 2

Optimum conditions of the ECF process (conventional and innovative) for removal of contaminants for different concentrations.

Feed number	Volume (ml)	Current density (mA/cm ²)	OT (min)	Stirring (rpm)	Initial pH	Final pH	Initial EC (mS/cm)	Final EC (mS/cm)
1	1300	9.32	70	400	8.9	9.04	4.7	3.5
2	1300	9.32	48	400	8.7	9.4	3.2	2.2
3	1300	9.32	32	400	8.8	9.4	2.3	1.5
4	1300	5.83	30	400	8.8	9.3	1.7	1.1
5	1300	5.83	20	400	8.9	8.97	1.7	1.4
6	1300	5.83	10	400	8.8	9.1	0.88	0.66

(OH)₃) and another proton (H⁺).

3.2. Removal efficiency of contaminants

In the ECF process, the removal efficiency of contaminants is affected by parameters such as current density (Chen et al., 2000), coagulant dosing rate (Holt et al., 2005), operating time, pH value (Jiang et al., 2002), concentration, and stirring speed (Ahmed et al., 2018). As stated in section 2.2, to consider the effect of initial concentration on the removal efficiency, the feed was diluted to prepare solutions with different concentrations as outlined in Table 1. Although the pH value was not affected by dilution, nevertheless, current density, operating time, and electro conductivity have profoundly been affected due to decrease in the contaminant concentration.

The extent of the chemical reaction can be expressed in terms of Faraday's law, through which, the mass of dissolved metal can be calculated theoretically. According to this law (see eq. (9)), the release of metal ions in electrocoagulation for the formation of metal complex (e.g. Al(OH)₃) as coagulant, is a function of current and operating time. Thus, to minimize energy demand and associated costs with the metal consumption, and also to prevent the re-stabilization of suspended particles, it was crucial to carefully determine the optimal conditions for current density and operating time, as defined below:

$$n = \frac{it}{zF} \quad (9)$$

in this equation, n is the mass of dissolved anode (g), i stands for the current (A), t is the electrolysis time (s), F represents the Faraday's constant (F = 96,500 C mol⁻¹), and z is the cation charge (z = +3 for Al or +2 for Fe) (Barrera Diaz et al., 2005) (Panizza and Cerisola, 2004).

Table 2 reports the optimum conditions of ECF (the same conditions for conventional and innovative) for removal of contaminants for different concentrations. The optimum conditions were attained in accordance with the maximum removal efficiency, when the exact dosage of coagulants would be released in the solution. Since the cell volume and electrode surface of conventional and innovative ECF are similar, then at optimum conditions, the operating parameters are also

similar. Spiral electrode configuration in cylindrical cell outperformed consistently when compared with the rectangular cell in terms of removal efficiencies. As a result of enhanced flow dynamics in the cylindrical setup, the coagulant (aluminium ions) was more evenly distributed throughout the feed (wastewater).

It is imperative to understand the underlying reactions when discussing electrocoagulation. The aluminium anode releases Al³⁺ ions into the wastewater. Hydrolysis reactions then form monomeric and polymeric species from these ions. By reacting with contaminants, these species destabilize them, enabling them to coagulate and be removed from the feed. As a result of the enhanced mixing in the cylindrical setup, these reactions occur more effectively, resulting in a higher removal rate. On the other hand, the conventional rectangular setup may not provide enough mixing, which would lead to zones where the coagulant concentration is not optimal, hence lower removal efficiency would be expected.

As presented in Table 2, the optimum current density for the diluted concentrations (feed 4, 5, and 6) was obtained to be 5.83 mA/cm² and for the higher concentrations (feed 1, 2, and 3), it was 9.32 mA/cm². The reader is referred to supplementary materials for the experimental data points that led to optimum values in this table. According to Faraday's law, the concentration of metal in the solution depends on operating time (hydrolysis time) and current. Thus, the operating time and Al³⁺ concentration decreased at lower concentrations. The evolution of pH is also presented in this table. It is noteworthy that EC can be utilized as a pH regulator because it increases the acidic pH and reduces the alkaline pH. In this study, although the initial pH is alkaline and the reduction of pH is expected, nevertheless, an increase in pH was observed. This contradiction can be attributed to the high concentration of particles and organics in the solution. Under such circumstances, the contaminants (e.g. SiO₂, organic matters) may partially react with anode electrode thus less coagulants are expected to form. This may, in turn, cause higher concentration of hydroxide ions in the solution. Fig. 5 presents the images of formed flocs in the settling tank and filtrated solution for different feed concentrations based on Table 1. As it can be seen, with the reduction of concentration from feed 6 to feed 1, the behaviour of sludge would also change. In feeds 5 and 6, due to the low concentration

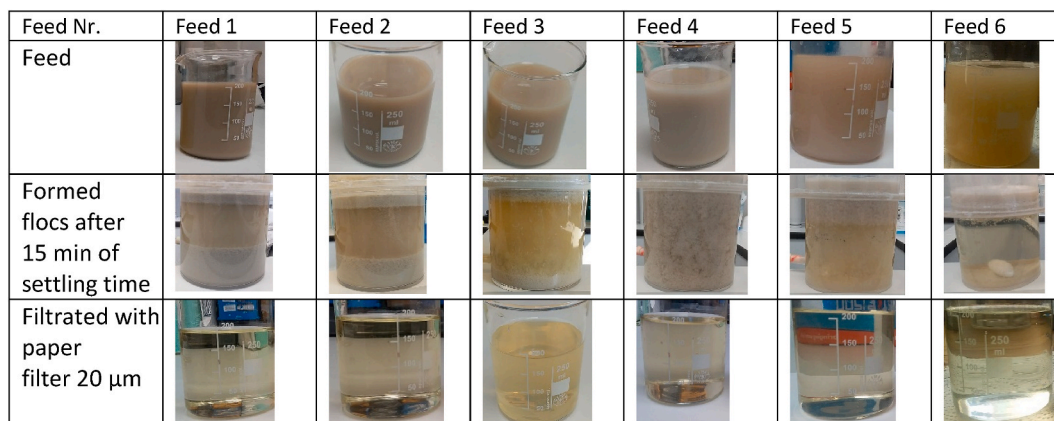


Fig. 5. Images of different feed concentrations (see Table 1), formed flocs and filtrated solutions.

Table 3
Comparison of contaminant removal efficiency between conventional and innovative ECF configurations (case study: Feed 1).

Parameters	Turbidity (NTU)	TOC (mg/L)	Si (mg/L)	Zn (mg/L)	Pb (mg/L)	Cu (mg/L)	Cr (mg/L)
Feed 1 (no dilution)	15,300	31,895	154.1	13.6	2.22	5.54	10.1
Treated with Conventional-ECF	839.0	14,515	41.70	1.66	0.43	0.82	1.92
Treated with Innovative-ECF	486.0	12,735	4.08	0.46	<0,10	0.16	1.22

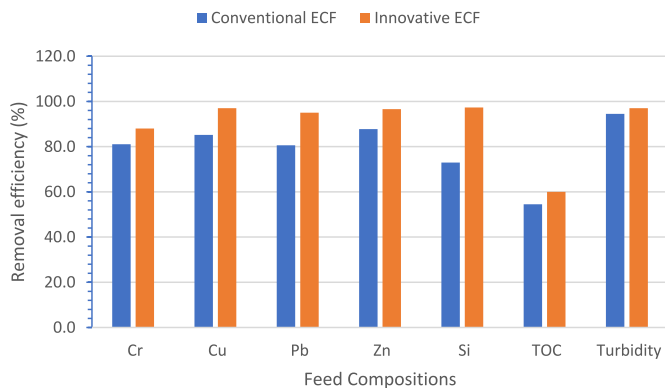


Fig. 6. Comparison of removal efficiency between conventional and innovative ECF configurations (case study: feed 1).

Table 4
Removal efficiency of contaminants for different concentrations in the innovative ECF configuration.

	Turbidity (NTU)	TOC (%)	Si (%)	Zn (%)	Pb (%)	Cu (%)	Cr (%)
Feed 1	97	60	97.3	96.6	95	97	88
Feed 2	98	54	98	96.2	94.2	93.6	86.5
Feed 3	98.7	65	99	98.7	97.6	97	92
Feed 4	98.6	64	98.6	99.3	98	90	98
Feed 5	98	40	95.5	99	96.5	93	91
Feed 6	99.7	69	97	99.2	93.2	95.4	93.5

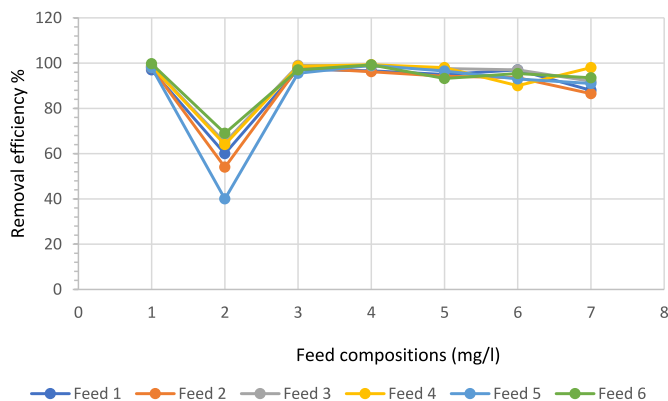


Fig. 7. Comparison of the removal efficiency for different concentrations in innovative ECF configuration 1: Turbidity, 2: TOC, 3: Si, 4: Zn, 5: Pb, 6: Cu, 7: Cr).

of impurities, the flocs with low density were formed which then floated on the surface of the solution. On the contrary, for feeds 1 and 2, as the concentration of impurities increases, the coarse flocs would be formed

so that the gravity force dominates which finally causes flocs to get settled. The latter is more effective in removal of heavy metals.

In removal of contaminants, the performance of spiral ECF was superior to the conventional one for all concentrations. For instance, the results of feed 1 were compared between the conventional and spiral ECF configurations which can be found in Table 3, and Fig. 6. The better performance of the cylindrical cell is mainly due to much more mixing between the coagulants and contaminants which resulted in higher efficiency of ECF. In other words, in the cylindrical ECF, the electrode configuration would propel coagulants and contaminants towards the center of the cell causing better mixing. In conventional ECF though, poor mixing is the prime drawback that causes lower removal efficacy (see section 3.3). These findings are consistent with those of Emamjomeh and Sivakumar (2009), who reported profound removal efficiency of electrocoagulation for various pollutants. However, the efficiency of spiral ECF system surpassed the one that is reported by Kobya et al. (2007), especially in the treatment of textile wastewaters.

The removal efficiency of contaminants for different concentrations, only for the cylindrical ECF, is also presented in Table 4 and Fig. 7. As it can be seen, although the tests for both cells have been carried out at the same conditions, for all concentrations (feeds 1–6), the removal efficiency is higher than the conventional one. This superiority can primarily be attributed to better flow condition in terms of better mixing due to electrode and cell configuration which also improved the mass transfer. Fig. 7 shows that compared to other contaminants, TOC was less efficiently reduced in both ECF configurations. This can be explained for two reasons: 1) pH effect and 2) high concentration of suspended solids. Once the pH value is higher than 8, then the removal efficiency of oil contents would be decreased. This occurrence has also been reported by Merma et al. (2020). They investigated the effect of pH value when it changed from 4 to 12 on removal of an oily wastewater from mining industry using electrocoagulation. They reported that the highest removal efficiency was obtained at pH 4.06 thus for oily wastewaters, pH should be lower than 8.1.

3.3. Effect of ECF configuration on flow hydrodynamic

Flow hydrodynamics in the reactor should be augmented to meet three principal expectations:

- 1) Removal of gas bubbles which may be generated on the cathode. If these gas bubbles remain on the electrode surface, then they may cause smaller electrode active surface. To keep the removal efficiency unchanged under such circumstances, then higher voltage would be required which implies excessive energy consumption.
- 2) Reduction of polarization phenomenon on the anode surface would be essential for the prevention of fouling (passivation). Increased turbulence and shear forces at higher flow rates can dislodge particles that tend to settle on electrode surfaces. This would, in turn, prevent fouling and maintains the efficiency of electrocoagulation processes.
- 3) Enhancement of mass transfer and better mixing between coagulants and contaminants.

The flow hydrodynamics in the cell cannot be enhanced only by stirring as it may otherwise cause higher energy consumption. Instead, the electrode configuration would play an important role. The disadvantage of conventional ECF, in which the plate electrodes are placed in

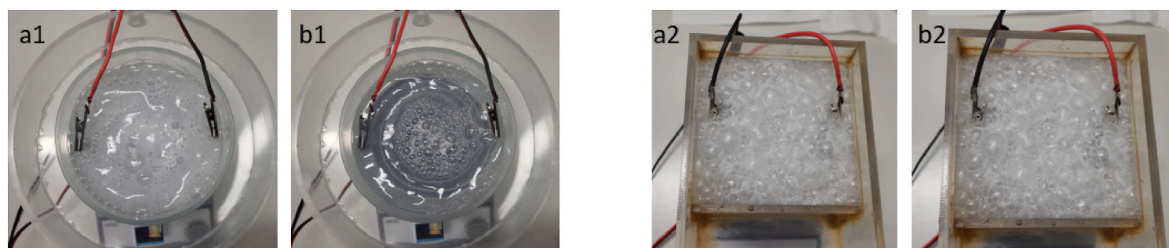


Fig. 8. Effect of stirring on removal of gas bubbles and foam in conventional and spiral configurations (a1, a2: no stirring), (b1, b2: stirring speed 400 rpm).



Fig. 9. A typical image of attached gas bubbles on the electrode surface in the conventional ECF (passive cathode).

a rectangular cell, is closely associated to the flow hydrodynamics between the electrodes which may not be sufficient to propel the contaminants to the cell surface. This can be related to the plate configuration, which would complicate the removal of gas bubbles or the reduction of polarization on the electrodes. Moreover, the dead zones in the corners of the rectangular cell are prone to lower mixing (Bayar et al., 2011), (Trinh et al., 2021).

To increase mixing in the ECF process, the spiral electrode configuration inside a cylindrical cell is expected to increase the flow velocity between electrodes, so then the mass transfer coefficient is anticipated to increase. This allows sufficient contact time between coagulants and

contaminants which may finally give rise to higher removal efficiency (see section 3.2). Naje et al. (Ahmed et al., 2019), investigated the enhancement of ionic mass transfer coefficient using electrocoagulation with rotating anode and reported that the mass transfer coefficient increases with the rotational speed.

In the course of laboratory tests in this work, similar behavior was also observed. Fig. 8 compares the conventional and spiral configurations for two different operating conditions of without and with stirring speed of 400 rpm. Fig. 8-a1 and 8-a2 show both ECFs when the stirring speed was zero. As it is evidently demonstrated, the foam and gas bubbles have covered the surface of both cells. On the contrary, Fig. 8-b1 and 8-b2 show that for the stirring speed of 400 rpm, the gas bubbles and foam were almost removed from the surface of the innovative ECF. Moreover, due to the centripetal force, the formed foam and gas bubbles tend to move toward the center of the cell. For the conventional ECF though no such behavior was observed. Fig. 9 shows that the gas bubbles would remain close to the electrode surface in the conventional ECF since the flow condition between the plates was not sufficient to remove the generated gas bubbles.

To confirm the experimental work and compare the flow hydrodynamic of the cylindrical ECF with the conventional one, a fluid flow simulation using Computational Fluid Dynamics (CFD) with similar dimensions and conditions, as those presented in Figs. 1 and 2, was performed (see Fig. 10). For the geometrical construction, the Ansys SpaceClaim environment was used. In general, to use the sliding mesh tool in Fluent, each cell in simulation was divided into two main parts, 1) a moving part (the space of stirring) and 2) out of the moving part (stationary part). Similar to experimental study, a water volume of 1300 ml was considered for both cells. Similar stirrer dimension and stirring speed of 400 rpm were considered for conventional and cylindrical ECF configurations. The flow model of “SST k-omega” was selected for the turbulent flow regime and the model of “Volume of Fluid (VOF)” was used to simulate two-phase (water and air) flow.

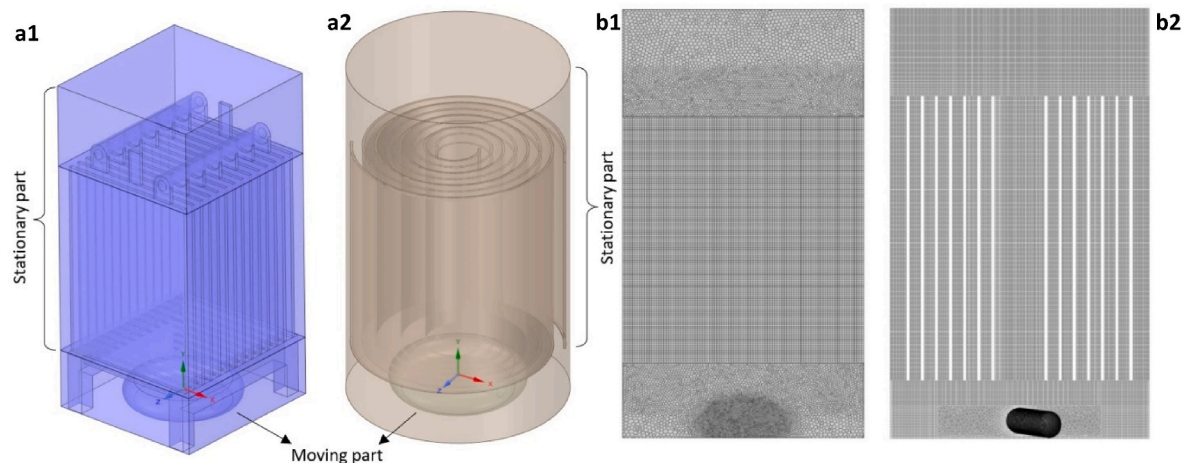


Fig. 10. The moving and stationary parts and the meshing system, determined for both configurations in Ansys Fluent, a1 and b1: conventional ECF, a2 and b2: Innovative ECF.

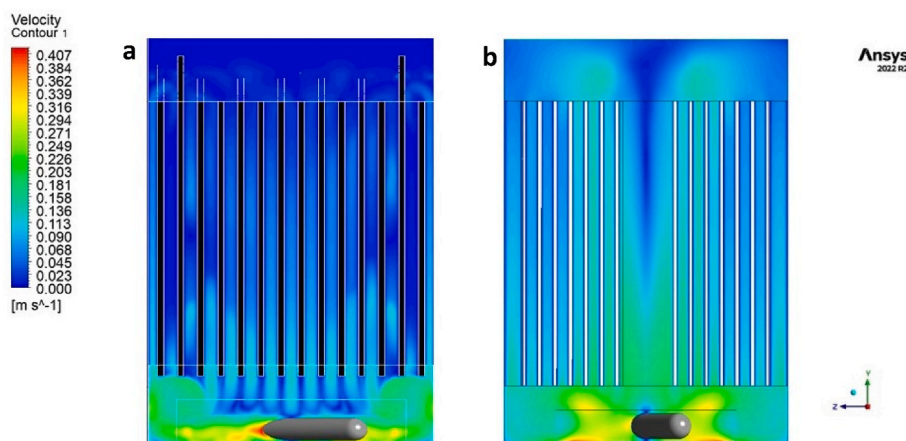


Fig. 11. The velocity contour of a) conventional ECF, b) Innovative ECF.

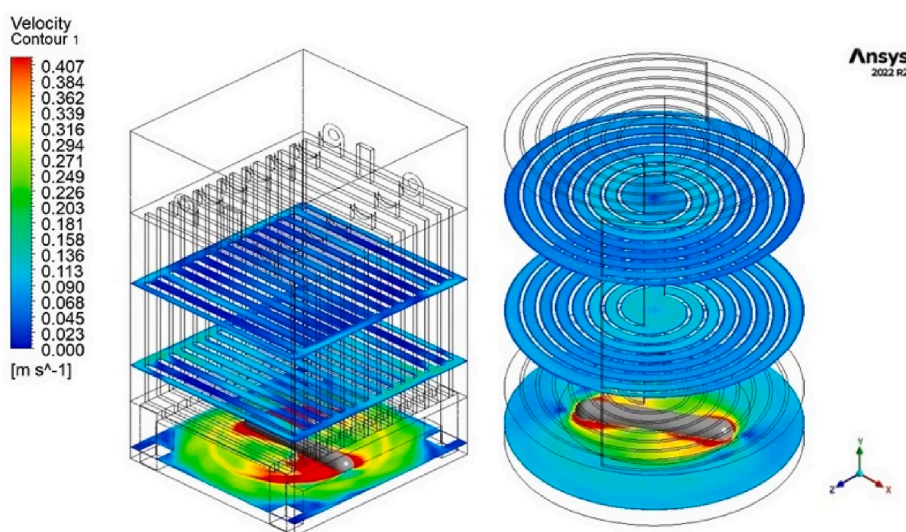


Fig. 12. The velocity contour in different vertical positions a) conventional ECF, b) Innovative ECF.

An efficient ECF configuration would preferably provide a uniform flow distribution between the electrodes. The comparison of flow velocity distribution between the conventional and cylindrical ECF configurations has been shown in Figs. 11 and 12. As it can be seen, the uniformity and velocity in the cylindrical ECF are greater than those in the conventional ECF. In the conventional ECF, the vertical plate electrodes serve as barrier against flow circulation, so then flow cannot be circulated and distributed evenly between the electrodes. This is a condition under which, fouling is anticipated to occur under the passivation of electrodes. Under such circumstances, fouling potential increases on the anode electrode and reduces the mass transfer coefficient. Moreover, the formed gas bubbles, which reduce the electrode surface on the cathode, cannot be pushed out, resulting in voltage increase and energy consumption (see also Fig. 9). It should be also pointed out that in cylindrical ECF, the enhanced flow velocity on the surface, would create vortices. They would, in turn, cause lower foam formation, while very slow flow on the surface of the conventional ECF led to much more foaming. This behavior was also observed during the laboratory tests (see section 3.5 and Fig. 14). The impact of flow hydrodynamics, as highlighted in this study, are consistent with the observations of Zodi et al. (2011), for the treatment of textile wastewater. However, the cylindrical configuration with spiral electrodes proved to be more effective in terms of mixing and turbulence that provided better removal of the contaminants from the cell.

3.4. Energy consumption and voltage rise

The cost of electrical energy (kWh m^{-3}) can be calculated from the following equation (Brahmi et al., 2019b):

$$C = U * I * \frac{t}{V} \quad (14)$$

where U is the voltage (V), I is the current (A), t is the time of electrolysis (h) and V is the volume (m^3) of solution. To reduce energy consumption, the voltage should be reduced as much as possible. High current increases ohmic drop (IR drop) and voltage between electrodes. IR drop results from the ohmic resistance of the electrolyte R , which can be explained as follows (Hakizimana et al., 2017):

$$R = \frac{l}{S} * \frac{1}{k} \quad (15)$$

where l is inter-electrode distance (cm) and k stands for the conductivity of electrolyte (mS/cm) and S is the electrode surface area (cm^2). According to this equation, higher conductivity decreases ohmic resistance that leads to lower energy consumption. Fekete et al. (2016) reported 2 mS/cm for reduction of the effect of conductivity on IR-drop. One of a key problem of EC process which increases cell voltage and energy consumption is the passivation of the cathode that can be avoided by optimization of flow pattern and the current reversal frequency (Hansen

Table 5
Energy consumption of different feed concentrations for innovative ECF.

Feed Nr.	Measured Al (g)	Al molar mass (g/mol)	Al Charge	F (C mol ⁻¹)	It (C)	Time (min)	Average V	Stirrer energy spent (kWh)	ECF Power Energy (kWh)	Total Energy (kWh)	Total Energy (kWh/m ³)
Feed 1	2.4	27	3	96500	25733	70	2.91	0.007	0.02	0.027	20.8
Feed 2	1.65	27	3	96,500	17691	48	3.135	0.0048	0.015	0.0198	15.2
Feed 3	1.14	27	3	96500	12223	32	3.22	0.0032	0.01	0.0132	10.2
Feed 4	0.63	27	3	96500	6755	30	3.59	0.003	0.006	0.009	6.9
Feed 5	0.46	27	3	96500	4932	20	3.1	0.002	0.004	0.004	4.6
Feed 6	0.22	27	3	96500	2358	10	4.08	0.001	0.0025	0.0035	2.67

F: Faraday's constant; C: Coulomb; V: Voltage; J: Joule.

Table 6
Voltage increase and metal consumption for different feed concentrations and operating times.

Feed number	Voltage (V)	Conventional ECF	Innovative ECF	Time (min)	Current (A)	Measured Al (g)	Calculated Al (g)
Feed 1	initial Voltage (V)	4.57	2.57	70	8	2.4	3.13
	Final Voltage (V)	5.7	3.26				
Feed 2	initial Voltage (V)	3.26	2.57	48	8	1.65	2.14
	Final Voltage (V)	4.33	3.7				
Feed 3	initial Voltage (V)	3.2	2.87	32	8	1.14	1.43
	Final Voltage (V)	4.58	3.57				
Feed 4	initial Voltage (V)	3.58	3.24	30	5	0.63	0.84
	Final Voltage (V)	5.45	3.94				
Feed 5	initial Voltage (V)	3.6	3.23	20	5	0.46	0.56
	Final Voltage (V)	3.07	2.97				
Feed 6	initial Voltage (V)	4.44	3.86	10	5	0.22	0.28
	Final Voltage (V)	5.19	4.30				

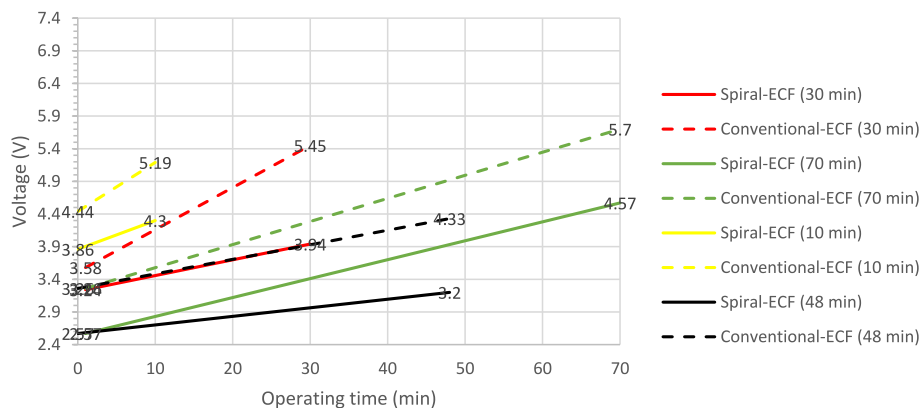


Fig. 13. Comparison of voltage increase for different feed concentrations and operating time of 10, 30, 48, and 70 min (Dash line: conventional ECF, solid line: innovative ECF).

et al., 2007). It should be stated though that the influence of the passivation layer on electrical resistance is a limitation of our model in this study. The energy consumption has been calculated in Table 5 based on the amount of metal (aluminium) released into the solution, as determined by Faraday's law (Eq. (9)):

$n = \frac{it}{zF} \rightarrow it = nzF$, (1 C (Electric charge) = 1A*1s), (C: coulomb, A: Amp, s: second).

Example: calculation of energy consumption for Feed 1 (innovative ECF):

$it = \left(\frac{2.4}{27}\right) * 3 * 96500 = 0.25 * 10^5$ C charge is needed in 70 min, i.e. ≈ 6 C/s.

Average voltage = $\frac{2.57+3.26}{2} = 2.91$ V.

The dissolution of 2.4 g Al requires $0.25 * 10^5$ C * 2.91 V = 0.072 MJ = 0.02 kWh electric energy for 1300 ml solution volume.

It should also be noted that a charge of 6 C/s correspond to a CD of 7 mA/cm², whereas, for feed 1, the CD of 9.32 mA/cm² has been used. This gap can be explained as the difference between the measured dissolved metal and the calculated one (see Table 6). The measured values

were lower than the calculated ones from the Faraday's law. This is because the Faraday's law assumes that all the supplied current could be passed through the cell and does not consider other factors that may affect metal dissolution such as the actual amount of current that passes through the cell (Cruz et al., 2019). Similar results have been reported elsewhere (Lima, 2019) (Naje et al., 2016) (Brahmi et al., 2019b) (Vepsäläinen et al., 2012) (Cruz et al., 2019). It should be noted that the mass of electrodes was not measured directly due to minimal and difficult-to-measure mass loss from the electrodes.

Fig. 13 compares the voltage rise between the conventional and spiral ECF configurations. In general, two reasons can be expressed for increasing voltage in ECF. Firstly, the formation of a passive film (gel layer) on the anode that develops resistance (Brahmi et al., 2019b), and secondly, on the cathode electrode, the hydrogen gas would be formed. The bubbles that insulate the cathode surface would then be generating an oxide film on the electrode surface (passivation effects). This problem increases the total electrical resistance and to attain the optimal removal results in excessive consumption of electrical energy (Martinez et al.,

Time (min)	Conventional ECF	Volume of foam (cm ³)	Innovative ECF	Volume of foam (cm ³)
After 5 min		23		5.6
After 10 min		76		8.4
After 15 min		153		14
After 20 min		228		85

Fig. 14. Comparison of produced foam after 5, 10, 15, and 20 min.

2000). As discussed in section 2.1, to address these problems and prevention of voltage rise, the flow hydrodynamic around the electrodes must be augmented for the bubbles to be pushed out and enhancement of mass transfer near the anode electrode (Mollah et al., 2004a). As shown in Fig. 13, while the electrolyte and operating conditions in both cells (conventional and innovative) were similar, nevertheless, lower voltage was experienced for all concentrations (feeds 1–6) for the spiral ECF. Mollah et al. (2004a) also underlined the importance of energy efficiency in electrocoagulation systems. Their results revealed that operating parameters, such as current density, would greatly influence the energy consumption. The spiral ECF design demonstrated a more efficient energy consumption. This becomes even more relevant when compared with the conventional systems, which have been reported to often consume more energy, especially at higher current densities, as noted by Emamjomeh and Sivakumar (2009).

3.5. Foaming

Aluminium hydroxide (Al(OH)₃) and hydrogen gas (H₂) could be formed during the ECF process (Landels et al., 2019). As soon as the flocs are generated, then the electrolytic gas bubbles in the liquid create a flotation effect. This, in turn, causes their density to be lower than the surrounding liquid, removing the pollutants to the floc-foam layer at the liquid surface (Mollah et al., 2004b) (Landels et al., 2019). The produced

foam on the liquid surface would then degrade the ECF efficiency due to the high volume of foam (Mohammadi et al., 2017).

Fig. 14 compares the generated foam after 5, 10, 15, and 20 min. Evidently, the rectangular ECF process had less effective stirring, leading to less mixing at the liquid surface. This is because the plate electrode acts as a barrier to flow circulation within the cell, resulting in the production of a uniform foam layer that can thicken over time. This thickening can substantially reduce the efficiency of the electrochemical process and may cause a sharp rise in voltage, thereby increasing energy consumption. Conversely, the enhanced flow dynamics in the cylindrical ECF lead to migration of gas bubbles to the cell centre which, in turn, generates small vortices in the central part of the cell. These phenomena reduce the rate of foam formation over time, thereby increasing the efficiency of the ECF process. It should finally be pointed out that this study primarily aimed at comparing the efficiencies of conventional and cylindrical ECF configurations, nonetheless a detailed analytical comparison, in terms of SEM, FTIR, XRD, etc., would also be imperative which is currently underway.

4. Conclusions

The main objective of this study was to develop a spiral electrode configuration for enhancing the functionality of the ECF process. The impact of this new configuration on the removal efficiency of

contaminants was also investigated for an industrial wastewater with different concentrations. The results were then compared with a conventional rectangular ECF. The following conclusions can be drawn from the results of this study:

- The spiral ECF configuration achieved a removal efficiency of approximately 90% under operating conditions attempted in this study. This has profoundly outperformed the conventional configuration.
- The spiral ECF configuration was almost 20% more energy-efficient for operating times ranging from 10 to 70 min. This implies a substantial reduction of energy costs.
- CFD (computational fluid dynamics) simulations revealed that the improved flow dynamics within the spiral ECF system led to considerably lower foam formation. This would, in turn, reduce the need for additional energy to maintain high cell efficiency.
- The findings indicate that the spiral electrode configuration can potentially improve the system efficiency in terms of contaminant removal and energy consumption when compared with those in rectangular ECF systems. Future work would involve the optimization of the spiral configuration and its application in a broader range of wastewater treatment.

Credit

Ehsan Jafari: Investigation, Methodology, Writing – original draft, Visualization, M. Reza Malayeri: Supervision, Methodology, Writing – review & editing, Heike Brückner: Resources, Methodology, Thomas Weimer: Resources, Methodology, Peter Krebs: Supervision, Methodology, Writing – review & editing.

Declaration of competing interest

The authors whose names are listed immediately below certify that they have no affiliations with or involvement in any organization or entity with any financial interest (such as honoraria; educational grants; participation in speakers' bureaus; membership, employment, consultancies, stock ownership, or other equity interest; and expert testimony or patent-licensing arrangements), or non-financial interest (such as personal or professional relationships, affiliations, knowledge or beliefs) in the subject matter or materials discussed in this manuscript.

Data availability

Data will be made available on request.

Acknowledgements

This study has been carried out within the framework of a doctoral thesis. The authors would like to thank Mr. Holger P. Haerter, head of Spiraltec GmbH in Sachsenheim, Germany, for supporting this study.

Appendix A. Supplementary data

Supplementary data to this article can be found online at <https://doi.org/10.1016/j.jenvman.2023.119085>.

References

Adhoum, N., Monser, L., 2004. Decolorization and removal of phenolic compounds from olive wastewater by electrocoagulation. *Chem. Eng. Process* 43, 1281–1287.

Ahmed, S.N., Al Khateeb, Raid T., Shreeshivadasan, 2018. Treatment of textile wastewater using a novel electrocoagulation reactor design. *Global NEST* 20, 449–457.

Ahmed, Samir, Naje, Ajeel, Mohammed A., Rahman Ismael, Mahdi, Alkhateeb, Raid T., Al-Zubaidi, Hussein A.M., 2019. Enhancement of ionic mass transfer coefficient using a unique electrocoagulation reactor with rotating impeller anode. *Separ. Sci. Technol.* 55, 1167–1176.

Bandaru, S.R.S., Roy, A., Gadgil, A.J., van Genuchten, C.M., 2020. Long-term electrode behavior during treatment of arsenic contaminated groundwater by a pilot-scale iron electrocoagulation system. *Water Res.* 175.

Barrera Díaz, C., Roa Morales, G., Ávila Córdoba, L., 2005. Electrochemical treatment applied to food-processing industrial wastewater. *Ind. Eng. Chem. Res.* 45, 34–38.

Barrera-Díaz, C., Bilyeu, B., Roa, G., Bernal-Martinez, L., 2011. Physicochemical aspects of electrocoagulation. *Separ. Purif. Rev.* 40 (1), 1–24.

Barrera-Díaz, C.E., Lugo-Lugo, V., Bilyeu, B., 2012. A review of chemical, electrochemical and biological methods for aqueous Cr (VI) reduction. *Hazard Mater* 223, 1–12.

Bayar, Serkan, Yalçın Şevki, Yıldız, Erdem Yılmaz, Alper, İrdemez, Şahset, 2011. The effect of stirring speed and current density on removal efficiency of poultry slaughterhouse wastewater by electrocoagulation method. *Desalination* 280, 103–107.

Brahmi, K., Bouguerra, W., Hamrouni, B., Elaloui, E., Loungou, M., Tlili, Z., 2015. Investigation of electrocoagulation reactor design parameters effect on the removal of cadmium from synthetic and phosphate industrial wastewater. *Arab. J. Chem.* 12, 1848–1859.

Brahmi, K., Bouguerra, W., Hamrouni, B., Elaloui, E., Loungou, M., Tlili, Z., 2019a. Investigation of electrocoagulation reactor design parameters effect on the removal of cadmium from synthetic and phosphate industrial wastewater. *Chemistry* 12, 1848–1859.

Brahmi, K., Bouguerra, W., Hamrouni, B., Elaloui, E., Loungou, M., Tlili, Z., 2019b. Investigation of electrocoagulation reactor design parameters effect on the removal of cadmium from synthetic and phosphate industrial wastewater. *Arab. J. Chem.* 12, 1848–1859.

Burns, S.E., Yiacoumi, S., Tsouris, C., 1997. Microbubble generation for environmental and industrial separations. *Sep. Purif. Technol.* 11, 221–232.

Canizares, P., Martinez, F., Jimenez, C., Saez, C., Rodrigo, M.A., 2008. Coagulation and electrocoagulation of oil-in-water emulsions. *Hazard. Mater* 151, 44–51.

Casqueira, R.G., Torem, M.L., Kohler, H.M., 2006. The removal of zinc from liquid streams by electroflotation. *Min. Eng.* 19, 1388–1392.

Chen, G., 2004. Electrochemical technologies in wastewater treatment. *Sep. Purif. Technol.* 38 (1), 11–41.

Chen, X., Chen, G., Yue, P.L., 2000. Separation of pollutants from restaurant wastewater by electrocoagulation. *Sep. Purif. Technol.* 19, 65–76.

Cruz, K.D., Mateo, N.M., Tangara, N.P., Almendrala, M.C., 2019. Reactor design optimization on the electrocoagulation treatment of sugarcane molasses-based distillery wastewater. *Earth and Environmental Science* 344, 012023.

Emamjomeh, M.M., Sivakumar, M., 2009. Review of pollutants removed by electrocoagulation and electrocoagulation/flotation processes. *J. Environ. Manag.* 90, 1663–1679.

Fekete, E., Lengyel, B., Cserfalvi, T., Pajkossy, T., 2016. Electrocoagulation: an electrochemical process for water clarification. *J. Electrochem. Sci. Eng.* 6 (1), 57–65.

García-Segura, S., Eiband, M.M.S.G., de Melo, J.V., Martínez-Huitle, C.A., 2017. Electrocoagulation and advanced electrocoagulation processes: a general review about the fundamentals, emerging applications and its association with other technologies. *Electroanal. Chem.* 801, 267–299.

Hakizimana, J.N., Gourich, B., Chafi, M., Stiriba, Y., Vial, C., Drogui, P., Naja, J., 2017. Electrocoagulation process in water treatment: a review of electrocoagulation modeling approaches. *Desalination* 404, 1–21.

Hansen, H.K., Nuñez, P., Raboy, D., Schippacasse, I., Grandon, R., 2007. Electrocoagulation in wastewater containing arsenic: comparing different process designs. *Electrochim. Acta* 52, 3464–3470.

Heidmann, I., Calmano, W., 2008. Removal of Zn(II), Cu(II), Ni(II), Ag(I) and Cr(VI) present in aqueous solutions by aluminum electrocoagulation. *Hazard. Mater* 152, 934–941.

Holt, P.K., Barton, G.W., Mitchell, C.A., 2005. The future for electrocoagulation as a localised water treatment technology. *Chemosphere* 59, 355–367.

Ingelsson, M., Yasri, N., Roberts, E.P.L., 2020. Electrode passivation, faradaic efficiency, and performance enhancement strategies in electrocoagulation—a review. *Water Res.* 187.

Jafari, E., Malayeri, M.R., Brückner, H., Krebs, P., 2023. Impact of operating parameters of electrocoagulation-flotation on the removal of turbidity from synthetic wastewater using aluminium electrodes. *Miner. Eng.* 193, 108007.

Jiang, J.Q., Graham, N., André, C., Kelsall, G.H., Brandon, N., 2002. Laboratory Study of Electro-Coagulation-Flotation for Water Treatment, vol. 36. *Water Res.*, pp. 4064–4078.

Kobya, M., Bayramoglu, M., Eyvaz, M., 2007. Treatment of the textile wastewater by electrocoagulation: economical evaluation. *Chem. Eng. J* 128, 155–161.

Landels, Andrew, Beacham, Tracey A., Evans, Christopher T., Carnovale, Giorgia, Raikova, Sofia, Cole, Isobel S., Goddard, Paul, Chuck, Christopher, Allen, Michael J., 2019. Improving electrocoagulation floatation for harvesting microalgae. *Algal Res.* 39, 101446.

Lima, F., 2019. Oilfield produced water treatment with electrocoagulation. Doctoral thesis 61.

Mansoorian, H.J., Mahvi, A.H., Jafari, A.J., 2014. Removal of lead and zinc from battery industry wastewater using electrocoagulation process: influence of direct and alternating current by using iron and stainless steel rod electrodes. *Sep. Purif. Technol.* 135, 165–175.

Martinez, S.A., Rodriguez, M.G., Barrera, C., 2000. A kinetic model that describes removal of chromium VI from rinsing waters of the metal finishing industry by electrochemical processes. *Water Sci. Technol.* 42 (5–6), 55–61.

Merma, Antonio G., Santos, Brunno F., Artur, S., Rego, C., Hacha, Ronald R., Torem, Maurício L., 2020. Treatment of oily wastewater from mining industry using

- electrocoagulation: fundamentals and process optimization. *Materials Research and Technology* 9 (6), 15164–15176.
- Mohammadi, M.J., Salari, J., Takdastan, A., Farhadi, M., Javanmard, P., Yari, A.R., Dobaradaran, S., Almasi, H., Rahimi, S., 2017. Removal of turbidity and organic matter from car wash wastewater by electrocoagulation process. *Desalination Water Treat.* 68, 122–128.
- Mollah, M.Y.A., Morkovsky, P., Gomes, J.A.G., Kesmez, M., Parga, J., Cocke, D.L., 2004a. Fundamentals, present and future perspectives of electrocoagulation, *Journal of Hazardous Materials. Hazardous Materials* 114, 199–210.
- Mollah, M.Y.A., Morkovsky, P., Gomes, J.A.G., Kesmez, M., Parga, J., Cocke, D.L., 2004b. Fundamentals, present and future perspectives of electrocoagulation. *J. Hazard Mater.* 114, 199–210.
- Mouedhen, G., M, Feki, De Petris Wery, M., Ayedi, H.F., 2008. Behavior of aluminum electrodes in electrocoagulation process. *Hazardous Materials* 150, 124–135.
- Müller, S., Behrends, T., van Genuchten, C.M., 2019. Sustaining efficient production of aqueous iron during repeated operation of Fe(0)-electrocoagulation. *Water Res.* 155, 455–464.
- Naje, A.S., Chelliapan, S., Zakaria, Z., Ajeel, M.A., Alaba, P.A., 2016. A review of electrocoagulation technology for the treatment of textile wastewater. *Rev. Chem. Eng.* 10, 1515.
- Noorzalila Muhammad, Niza, Ijanu Emmanuel, Madu, Abdubaki Mohamed Hussen, Shadi, Suffian Mohd Yusof, Mohd, Anuar Kamaruddin, Mohammad, 2019. Role of turbulent flow and gas bubbles in enhancing mass transfer in batch electrocoagulation: a brief review. *Desalination Water Treat.* 161, 35–47.
- Panizza, M., Cerisola, G., 2004. Electrochemical oxidation as a final treatment of synthetic tannery wastewater. *Environ. Sci. Technol.* 38, 5470–5475.
- Phalakornkule, C., Polgumhang, S., Tongdaung, W., Karakat, B., Nuyut, T., 2010. Electrocoagulation of blue reactive, red disperse and mixed dyes, and application in treating textile effluent. *Environ. Manag.* 91, 918–926.
- Poon, C., 1997. Electroflotation for groundwater decontamination. *J. Hazard Mater.* 55, 159–170.
- Solak, M., Kilic, M., Yazici, H., Sencan, A., 2009. Removal of suspended solids and turbidity from marble processing wastewaters by electrocoagulation: comparison of electrode materials and electrode connection systems. *Hazard. Mater* 172, 345–352.
- Trinh, D.T., Quach, A.B., Ty, T.V., Channei, D., Nakaruk, A., Khanitchaidecha, W., 2021. Evaluation of magnetic stirring and aeration on electrocoagulation performance in actual industrial treatment. *Front. Environ. Sci.* 9.
- Ugurlu, M., Gurses, A., Dogar, C., Yalcin, M., 2008. The removal of lignin and phenol from paper mill effluents by electrocoagulation. *Environ. Manag.* 87, 420–428.
- Vepsäläinen, Mikko, Pulliainen, Martti, Sillanpää, Mika, 2012. Effect of electrochemical cell structure on natural organic matter (NOM) removal from surface water through electrocoagulation (EC). *Sep. Purif. Technol.* 99, 20–27.
- Vik, E.A., Carlson, D.A., Eikum, A.S., Gjessing, E.T., 1984. Electrocoagulation of potable water. *Water Res.* 18, 1355–1360.
- Zidane, F., Droguin, P., Lekhlif, B., Bensaid, J., Blais, J.F., Belcadi, S., El kacemi, K., 2008. Decolourization of dye-containing effluent using mineral coagulants produced by electrocoagulation. *Hazard. Mater* 155, 153–163.
- Zodi, S., Potier, O., Lapique, F., Leclerc, J.P., 2011. Treatment of the textile wastewaters by electrocoagulation: effect of operating parameters on the sludge settling characteristics. *Sep. Purif. Technol.* 81 (1), 62–68.
- Zongo, I., Maiga, A.H., Wethe, J., Valentin, G., Leclerc, J.P., 2009. Electrocoagulation for the treatment of textile wastewaters with Al or Fe electrodes: compared variations of COD levels, turbidity and absorbance. *Hazard. Mater* 169, 70–76.